

Data-Driven Approach for Parameter Estimation and Control of an Autonomous Underwater Vehicle

✉ Tabassum Rasul, ✉ Koena Mukherjee

National Institute of Technology Silchar, Department of Electronics and Instrumentation Engineering, Silchar, India

Abstract

This paper showcases a data-driven non-linear adaptive controller design employing an unfalsification approach to attain optimal estimates for unknown parameters in an autonomous underwater vehicle (AUV). These estimates are applied to the controller to enable precise trajectory tracking. The controller design presented is capable of adapting to parametric changes and uncertainties while fulfilling the desired performance criteria using an effective parameter update method of unfalsification. The results were validated through simulations conducted using MATLAB/SIMULINK.

Keywords: Adaptive control, Autonomous underwater vehicle, Data-driven control, Unfalsified control

1. Introduction

A complex non-linear dynamical system like autonomous underwater vehicle (AUV) undergoes changes in environmental conditions throughout its operation. In addition, the effects of added mass, which is the additional inertia encountered when a body accelerates through a fluid, must be accounted for while describing the dynamic equations. This causes uncertainty in the system parameters. As a result, modeling an AUV system accurately becomes an error-prone task. In addition, the presence of environmental disturbances like waves and ocean currents makes the process of AUV modeling even more difficult. Therefore, AUV control remains an ongoing research topic, and all the latest advancements in control methodologies are being tested on AUVs. These methodologies include robust control techniques, as seen in [1-3], adaptive control methods, as explored by [4], and optimal control, as demonstrated in [5], among others, which were applied to AUVs to obtain better performance in navigation and communication. Disturbance observer-based control methods have also been employed to address environmental disturbances, as evident in [6,7]. In the current scenario, researchers are increasingly drawn toward data-driven methods looking for alternatives

to model-based techniques, as relying on model-based techniques for controlling non-linear dynamic systems like AUV systems comes with plenty of assumptions. This paper introduces a data-driven method rooted in the unfalsification theory, which was initially devised by Safonov and Tsao [8] in 1995. It is an iterative procedure that relies on the system's input and output values. Unfalsified control theory is a supervisory technique in which the system is adapted to different scenarios by switching between controllers from among a finite set of candidate controllers. Controllers that meet the specified performance criteria are integrated into the closed-loop control system, whereas those that fail are excluded.

This method differs from gain scheduling, which relies on predefined controller gains without feedback to compensate for inaccuracies in scheduling and is a model-dependent technique [9,10]. Unfalsified control, on the contrary, evaluates the candidate controller a priori using the concept of fictitious reference and past measurement data and performs the selection procedure online. At any point in time, if the present controller fails to satisfy the desired criteria, it is removed from the loop and the next best candidate is brought into the loop. This method was applied to a 2-degree-of-freedom (DOF) robotic arm



Address for Correspondence: Tabassum Rasul, National Institute of Technology Silchar, Department of Electronics and Instrumentation Engineering, Silchar, India
E-mail: tabassum_rs@ei.nits.ac.in
ORCID ID: orcid.org/0000-0002-4456-7442

Received: 19.10.2023

Last Revision Received: 09.02.2024

Accepted: 22.03.2024

To cite this article: T. Rasul, and K. Mukherjee, "Data-Driven Approach for Parameter Estimation and Control of an Autonomous Underwater Vehicle." *Journal of ETA Maritime Science*, vol. 12(2), pp. 144-155, 2024.



Copyright © 2024 the Author. Published by Galenos Publishing House on behalf of UCTEA Chamber of Marine Engineers. This is an open access article under the Creative Commons Attribution-NonCommercial 4.0 International (CC BY-NC 4.0) License.

system for parameter estimation in [11]. The mathematical framework of this method and its several properties have been explored in [12]. The method was also tested for robustness in [13], and its stability properties were analyzed in [14]. In [15,16], the concept of unfalsification is combined with model reference adaptive control for set point tracking. It has been stated that the selection of an unfalsified controller may be performed either from a fixed set of candidates or via online optimization techniques. The online optimization technique was inspected in [17]. Furthermore, the control design was tried on a knee joint for the process of neuroprostheses in [18]. In [19], it was applied to a reactor system for temperature control. In a previous study, the application of this method to dynamic positioning in an AUV system was discussed [20]. In addition, data-driven methods have found utility in sample collection for oceanographic studies [21,22]. The design of a data-driven H_∞ loop shaping controller is detailed in [23], and more recently, its examination in non-linear time-varying plants is presented in [24-26].

1.1. Symbols and Abbreviations

$[]^T$ denotes the transpose of a matrix, $\| \cdot \|$ represents the Euclidean norm of the signal, and \int indicates the integration of a function. J is a rotation matrix determined by a choice of Euler angles, and \mathfrak{J} is the cost function, which depends on the system output, control input, and a fictitious reference. L_{2e} represents the extended Euclidean norm space and $\| \cdot \|_\tau$ denotes the truncated norm. Further details on these concepts are explored in the forthcoming sections.

The SNAME notation, as presented in [27], is adopted for describing the motion of AUVs in six DOF. Specifically, as illustrated in Figure 1, linear motion along the X-axis is denoted by x , while rotational motion along the X-axis is denoted by ϕ . Along the Y-axis, linear motion is denoted by y and rotational motion is denoted by θ . Along the Z-axis, linear motion is denoted by z , and rotational motion is denoted by ψ .

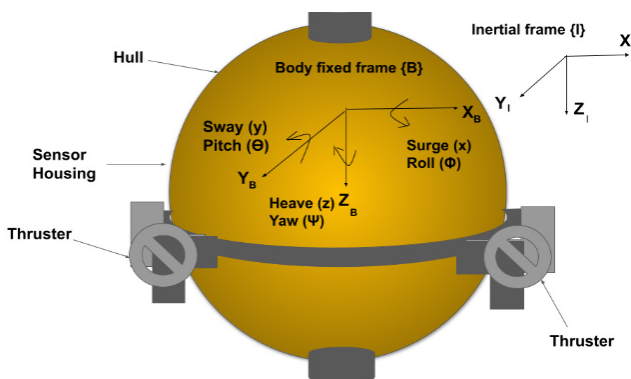


Figure 1. Position and angle representation in the reference frames

1.2. Structuring the Paper

The paper is structured as follows: Section 2 provides a summary of the AUV system and its mathematical model. Section 3 outlines the problem statement, and the adaptive unfalsified controller design is expounded in section 4. The stability analysis of the controller design is shown in Section 5. Section 6 discusses the simulation results, and the conclusion is presented in Section 7.

2. System Description and Model of the AUV

2.1. Construction of an AUV

An AUV is a propeller-driven platform commonly powered by lithium-ion batteries for propulsion. The key elements in the structure of an AUV encompass a hull, a propulsion system, a submersion mechanism, an electric power supply, navigation sensors, and a communication system. The AUV incorporates navigation sensors such as the inertial measurement unit (IMU) and sonar. In addition, it is equipped with pressure sensors, temperature sensors, battery monitoring sensors, leakage sensors, etc.

For AUVs, a pressure hull is essential to house its components in a dry, watertight environment. This hull accommodates electronic components and facilitates access for maintenance or modifications.

The volume of the AUV remains constant underwater, necessitating an increase in the downward force to dive deeper and counteract buoyancy. This can be achieved by adding mass through ballast tanks or external thrusters. Ballasting, which involves pumps and compressed air, is a common method, whereas thrusters pointing downwards offer a simpler but less power-efficient alternative.

All AUVs require propulsion, with motors being the prevalent choice due to their availability and cost-effectiveness. The placement of the motors affects the controllability across various DOF. Power consumption increases significantly with vehicle speed, posing an optimization challenge for achieving an ideal speed within the limited energy supply. Sealed batteries are used to supply electric power in AUVs.

Common methods for AUV navigation include dead reckoning, inertial navigation using IMUs, and acoustic navigation. However, to enhance the accuracy of inertial navigation sensors like IMU, additional aids such as differential global positioning systems for position estimation, Doppler velocity logs for velocity estimation, and pressure sensors for depth estimation are necessary. Acoustic navigation relies on the acoustic signals from the AUV transponder to determine its position. The primary methods used are long baseline and ultra-short baseline.

Underwater wireless communication in AUVs is usually achieved using acoustic communication. Acoustic modems are used for transmitting and receiving signals underwater. AUVs are developed in different shapes and sizes, each equipped with a different number of thrusters. The most common configurations include cylindrical or torpedo-shaped models, such as the REMUS and HUGIN, and spherical-shaped models like the ODIN.

The AUV under consideration in this study has a spherical model configuration, as shown in Figure 1. It comprises a closed spherical body featuring eight thruster assemblies to propel the vehicle and provide six DOF motion capabilities. In the autonomous mode, the vehicle is controlled by an on-board computer, whereas in the manual mode, control can be achieved by connecting to a ground station computer via TCP/IP through a tether. The tether, in autonomous mode, serves for monitoring and safety purposes. The sensor housing encloses the usual sensors for navigation and position estimation. In addition, other sensors such as oxygen or pH sensors are included based on the application of the designed AUV.

2.2. Mathematical Model and its Properties

Analyzing an AUV requires consideration of two reference frames, the body-fixed frame {B} and the inertial frame {I}, as illustrated in Figure 1. The mathematical model of the AUV characterizes its motion along various axes in 6 DOF through Euler angles.

The vehicular velocities with respect to the inertial frame (η) are described in relation to the velocities relative to the body-fixed reference frame (v) by [27]

$$\dot{\eta} = J(\eta)v \quad (1)$$

$$\text{Here } \eta = [\eta_1^T, \eta_2^T]^T = [x, y, z, \varphi, \theta, \psi]^T$$

$$\text{and } v = [v_1^T, v_2^T]^T = [u, v, w, p, q, r]^T$$

x, y, z represent linear displacements and φ, θ, ψ represent angular displacements in the inertial frame. Similarly u, v, w represent linear velocities and p, q, r represent angular velocities in the body fixed frame. $J(\eta)$ is the transformation matrix.

The dynamic model of an AUV considers hydrostatics, hydrodynamic forces, viscous damping, and propulsion forces and torques that act on the vehicle's body. The additional force due to the added mass is also accounted for. These components are encompassed in the non-linear hydrodynamic equation of motion of the AUV and are represented as;

$$M(\eta)\ddot{\eta} + C(\eta, \dot{\eta})\dot{\eta} + D(\eta, \dot{\eta})\dot{\eta} + g(\eta) = T + T_E \quad (2)$$

In the above equation, $M(\eta)$ represents the matrix containing mass and inertia coefficients, $M \in R^{6 \times 6}$, $C(\eta, \dot{\eta})$ signifies the Coriolis matrix, $C(\eta, \dot{\eta}) \in R^{6 \times 6}$, $D(\eta, \dot{\eta}) \in R^{6 \times 6}$ denotes the damping matrix, $g(\eta) \in R^6$ represents the gravitational matrix, T_E accounts for disturbances induced by environmental factors and $T \in R^6$ is the control input in the inertial reference frame encompassing both propulsion forces and torques. When the vehicle is fully actuated, the control input vector T can be expressed as

$$T = [T_x, T_y, T_z, T_\varphi, T_\theta, T_\psi]^T \quad (3)$$

The work presented in this paper focuses on an AUV with 4 DOF motion. The dynamic equation is given by

$$M\ddot{\eta} + D(\eta, \dot{\eta})\dot{\eta} = T + T_E \quad (4)$$

Here $\eta = [x, y, z, \psi]^T$ and $\eta, \dot{\eta}, \ddot{\eta} \in R^4$, $M \in R^{4 \times 4}$, $D(\eta, \dot{\eta}) \in R^{4 \times 4}$, T and $T_E \in R^4$.

Note:

N1. Here, the gravitational term is presumed to be zero given the constant desired motion along the Z-axis. The Coriolis and centripetal force terms are considered negligible due to the low speed of the vehicle and hence are omitted from the equation.

N2. The reference trajectory is expressed in the inertial frame; therefore, for mathematical gravity, the dynamical equation of the AUV is expressed in the same frame.

2.2.1. Properties

P1. The mass and inertia matrix is a positive definite symmetric matrix.

$$\delta_m I_n \leq M(\eta) \leq \delta_M I_n, \quad n = 1, 2, \dots, 6 \quad (5)$$

δ_m, δ_M are positive constants and I_n is the identity matrix of the n th order.

P2. The Damping matrix is non-symmetric and strictly positive definite.

$$D(\eta, \dot{\eta}) > 0 \quad (6)$$

The AUV model in Equation (4) is assumed to have unknown parameters; therefore, the mass and damping matrices are expressed in regressor form as;

$$Y(\eta, \dot{\eta}, \ddot{\eta})\Phi = T + T_E \quad (7)$$

where $Y(\eta, \dot{\eta}, \ddot{\eta}) \in R^{4 \times p}$ is a known regressor matrix and $\Phi = [\phi_1, \dots, \phi_p]^T$ is the unknown parameter vector.

3. Problem Description

3.1. Problem Statement

Given an input-output set $D_\tau = \{T_\tau, \Upsilon_\tau\}$ such that $D_\tau \in \mathfrak{L}_{2e}$ of the AUV system in (7) has uncertain parameters, the proposed adaptive unfalsified controller drives the AUV to follow a desired trajectory.

To realize this problem statement, the following assumption is required.

Assumption: The input-output data of the system, T and $\Upsilon = [\eta, \dot{\eta}, \ddot{\eta}]$ are measurable and available.

With the above assumption, the input-output data of the system are used to design the controller according to the proposed design. Because an infinite signal cannot be measured in real time, the input-output data of the system is truncated over a finite time.

Lemma 1: A truncated signal x_τ is defined as the signal $x(t)$ for a time period $\tau \in R$, if

$$x_\tau = \begin{cases} x(t), & t \in [0, \tau] \\ 0, & \text{otherwise} \end{cases}$$

A truncated L_2 norm of a truncated signal x_τ is given as

$$\|x\|_\tau = \int_0^\tau |x(t)|^2 dt$$

Here $\|x\|$ stands for the Euclidean norm of $x(t)$ for time τ . Also $x \in L_{2e}$ if $\|x\|_\tau$ exists $\forall \tau < \infty$ where L_{2e} is the extended L_2 norm space.

The AUV system (4) is simulated and run such that the input $T_T = T(t)_{t=0}^\infty$ when fed to the system generates the corresponding output $\Upsilon_T = \Upsilon(t)_{t=0}^\infty$ which is measured. This dataset $D_T = \{T_T, \Upsilon_T\}$ is truncated up to a period $t \in [0, \tau]$ to obtain the resultant set $D_\tau = \{T_\tau, \Upsilon_\tau\}$ and $D_\tau \in L_{2e}$. For mathematical simplicity the subscript τ is removed from the resultant data set $D_\tau = \{T_\tau, \Upsilon_\tau\}$, which is referred to as $\{T, \Upsilon\}$ from here on in the paper.

4. Controller Design

Unfalsified control is a data-based supervisory control technique that offers the advantages of both a robust and an adaptive control method. Non-linear systems like AUVs are affected mainly by parametric uncertainties and environmental disturbances. Thus, it is favorable to resort to a model-independent control method that is adaptive and can also tackle disturbances and non-linearities. Figure 2 illustrates the block diagram of the controller design.

4.1. Unfalsified Control Design

The closed loop structure in Figure 2 consists of the AUV system, whose parameters are not certain, a controller bank $C_B = [C_1, C_2, \dots, C_n]$ of n non-linear controllers designed using randomly chosen parameter values from a finite set within a given bound. The input from the controller and the output from the system are available for measurement. The unfalsified control method uses the measured data in iterations to find the most suitable controller from the aforementioned controller bank. To achieve this, a switching algorithm is devised. Controllers meeting the specified performance criteria are incorporated into the closed-loop system, whereas those falling short of the criteria are excluded. This is achieved by generating a fictitious

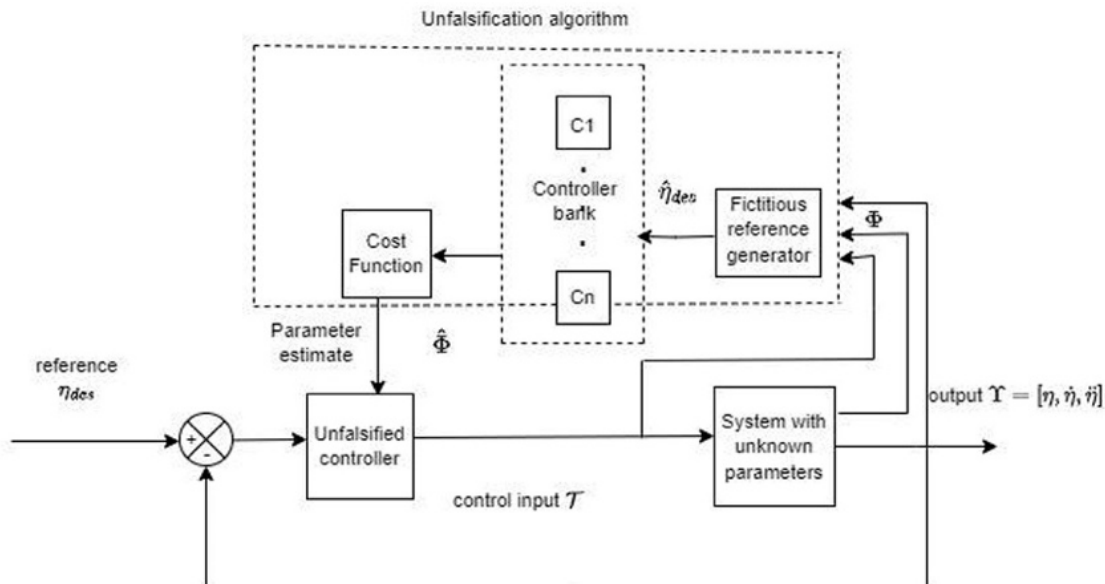


Figure 2. Adaptive unfalsified control system design

reference signal by which the controllers are evaluated by mathematical computation and are not required to be placed in the closed loop. Only the selected controller is placed in the closed-loop system.

The following terms are defined for comprehension.

D1: Fictitious Reference: A virtual signal that, if it were part of the closed loop system, would have generated the given set of input-output values for a specific controller is called the fictitious reference signal. For input T and output Y the fictitious reference can be computed as [28].

$$\hat{\eta}_{des} = C^{-1}T + Y \quad (8)$$

D2: Cost Function: To govern the system's performance and stability criteria, a function incorporating the system's input, output, and fictitious reference is defined as the cost function. All candidate controllers aim to minimize this cost function. The cost detectability property (Lemma 4 in section 4.4 of the paper) associated with the cost function ensures the closed-loop stability of the unfalsified controller [28].

4.2. Adaptive Unfalsified Control Design

The control problem is to design an adaptive unfalsified controller that allows the AUV to track a desired trajectory in the presence of parameter uncertainties and external disturbances without using explicit model information. The controller design is segmented into three stages.

Stage 1: A non-linear controller like a computed torque controller (CTC) is constructed, assuming all the parameters of the AUV system are known. Consider the difference between the desired and actual positions as the error given by

$$e_\eta = \eta_{des} - \eta \quad (9)$$

The control input obtained from the CTC is given by

$$T = M[\ddot{e}_\eta + \Lambda_1 \dot{e}_\eta + \Lambda_2 e_\eta] + M\ddot{\eta} + D(\eta, \dot{\eta})\dot{\eta} \quad (10)$$

Λ_1 and Λ_2 are positive gains that determine the speed of convergence of the tracking error to zero. Putting the value of T in equation (4), we obtain,

$$M\ddot{\eta} + D(\eta, \dot{\eta})\dot{\eta} = M[\ddot{e}_\eta + \Lambda_1 \dot{e}_\eta + \Lambda_2 e_\eta] + M\ddot{\eta} + D(\eta, \dot{\eta})\dot{\eta} + T_E \quad (11)$$

Stage 2: A set of n random values for unknown parameters forms the candidate set of controllers.

$$Y(\eta, \dot{\eta}, \ddot{\eta})\Phi = M[\ddot{e}_\eta + \Lambda_1 \dot{e}_\eta + \Lambda_2 e_\eta] + M\ddot{\eta} + D(\eta, \dot{\eta})\dot{\eta} + T_E \\ = M[\ddot{e}_\eta + \Lambda_1 \dot{e}_\eta + \Lambda_2 e_\eta] + Y(\eta, \dot{\eta}, \ddot{\eta})\Phi_i + T_E, \quad i = 1, 2, \dots, n.$$

Stage 3: Using the method of unfalsification, near-optimal values are estimated for the unknown parameters, and the CTC with the estimated parameters is inserted into the feedback loop. The CTC takes care of the trajectory tracking by the AUV.

Let the unknown mass matrix M be approximated as \hat{M} , an assumption for the bound of \hat{M}^{-1} is made. By property P1, M is positive definite and symmetric. Therefore, \hat{M}^{-1} exists and

$$0 < \hat{M}^{-1} \leq \Delta_{im} \quad (12)$$

where Δ_{im} is a positive. Hence, using the method of unfalsification, the unknown parameter Φ is estimated as $\hat{\Phi}$. The control law is modified to

$$T = \hat{M}[\ddot{e}_\eta + \Lambda_1 \dot{e}_\eta + \Lambda_2 e_\eta] + Y(\eta, \dot{\eta}, \ddot{\eta})\hat{\Phi} + T_E \quad (13)$$

Using Equations (7) and (13) the system dynamics thus becomes

$$Y(\eta, \dot{\eta}, \ddot{\eta})\Phi = \hat{M}[\ddot{e}_\eta + \Lambda_1 \dot{e}_\eta + \Lambda_2 e_\eta] + Y(\eta, \dot{\eta}, \ddot{\eta})\hat{\Phi} + T_E \quad (14)$$

which implies

$$\hat{M}[\ddot{e}_\eta + \Lambda_1 \dot{e}_\eta + \Lambda_2 e_\eta] + Y(\eta, \dot{\eta}, \ddot{\eta})\hat{\Phi} - Y(\eta, \dot{\eta}, \ddot{\eta})\Phi + T_E = 0 \quad (15)$$

$$\hat{M}[\ddot{e}_\eta + \Lambda_1 \dot{e}_\eta + \Lambda_2 e_\eta] + Y(\eta, \dot{\eta}, \ddot{\eta})e_\Phi + T_E = 0 \quad (16)$$

where $e_\Phi = \hat{\Phi} - \Phi$ is the estimation error.

$$\ddot{e}_\eta + \Lambda_1 \dot{e}_\eta + \Lambda_2 e_\eta + \hat{M}^{-1}Y(\eta, \dot{\eta}, \ddot{\eta})e_\Phi + \hat{M}^{-1}T_E = 0 \quad (17)$$

$$\ddot{e}_\eta = -\Lambda_1 \dot{e}_\eta - \Lambda_2 e_\eta - \hat{M}^{-1}Y(\eta, \dot{\eta}, \ddot{\eta})e_\Phi - \hat{M}^{-1}T_E \quad (18)$$

In matrix form

$$\begin{bmatrix} \dot{e}_\eta \\ \ddot{e}_\eta \end{bmatrix} = \begin{bmatrix} 0 & 1 \\ -\Lambda_2 & -\Lambda_1 \end{bmatrix} \begin{bmatrix} e_\eta \\ \dot{e}_\eta \end{bmatrix} + \begin{bmatrix} 0 \\ -\hat{M}^{-1}Y(\eta, \dot{\eta}, \ddot{\eta})e_\Phi - \hat{M}^{-1}T_E \end{bmatrix} \quad (19)$$

Equation (19) constitutes the error dynamics of the system. The closed-loop stability analysis is discussed in the next section. Once the control law is designed according to Equation (13), a fictitious reference (8) is computed for each controller of the bank as

$$\ddot{\eta}_{des} + \Lambda_1 \dot{\eta}_{des} + \Lambda_2 \eta_{des} = \hat{M}^{-1}[T + T_E + \hat{M}(\Lambda_1 \dot{\eta} + \Lambda_2 \eta) - \hat{D}(\phi, \eta, \dot{\eta})\dot{\eta}] \quad (20)$$

\hat{M}, \hat{D} represents mass matrix and damping matrix estimates. This fictitious reference is used to evaluate the cost function that determines the selection of controllers.

Note: N3. The controller inverse, in this case, requires the inverse of the mass matrix, which is invertible and bounded as given in Equation (12).

4.3. Algorithm of Unfalsification

The hysteresis algorithm applied for the falsification procedure involves the following steps:

1. Given input and output data $D_\tau = \{T, Y\}$ of the system with initial states.

2. for $i = 1, 2, \dots, n$, Formulate control law using (13) to constitute the candidates of the controller bank

$$C_B = [C_1, C_2, \dots, C_n].$$

3. Compute the fictitious reference $\hat{\eta}_{des}$ (20) for C_i .

4. Calculate the fictitious error $\hat{e}_{\eta_i} = \hat{\eta}_{des} - \eta$ for C_i .

5. Evaluate the performance of C_i by minimizing the cost function \mathfrak{J} given in Equation (30). Let at $\tau = 0$, $C = C_{initial}$ and $\mathfrak{J} = \mathfrak{J}_{initial}$

6. if for i^{th} iteration $\mathfrak{J}_i < \mathfrak{J}_{initial}$ then $\mathfrak{J} = \mathfrak{J}_i$ and $C = C_i$
else $C = C_{initial}$

End if

7. Increment i .

8. End for

9. Repeat steps 4 to 6 to find the arg min \mathfrak{J} .

10. Terminate when the minimum J is achieved.

C is the controller that remains unfalsified and runs in the closed loop system.

4.4. Stability Analysis and Proof

To establish the stability of an adaptive unfalsified controller, knowledge of a few relevant terms is required. These are defined as follows:

Lemma 2: The control problem is deemed feasible for a system S_ζ if there exists at least one stabilizing controller in the bank of candidate controllers C_B at any point in time [29].

Lemma 3: Unfalsified Stability: The stability of the system S_ζ is considered falsified by the data (T, Y) if

$$\sup_{\tau \in L_{2e}, \|T\| \neq 0} \frac{\|Y\|_\tau}{\|T\|_\tau} < \infty \quad (22)$$

Otherwise, the stability of the system S_ζ is asserted to be falsified by the input-output pair (T, Y) [29].

T1: Stability Theorem: Given a plant in (7) and a bank of controllers $C_B = [C_1, C_2, \dots, C_n]$ with at least one stabilizing controller as in (13), the closed loop system is said to be stable if the unfalsified controller minimizes the cost function $\mathfrak{J}(t)$ which satisfies the cost detectability property.

Proof: To prove closed-loop stability in an unfalsified control approach, we must meet the following three conditions. First, there must be at least one stabilizing controller in the controller bank. Second, an iterative algorithm leading to a finite number of switches is necessary. Finally, the cost function considered must satisfy the cost detectability property. According to the stability theorem stated above, it is imperative to demonstrate the stability of at least one candidate controller to fulfill the feasibility (Lemma 2) of the control problem.

Let system (7) lies in the space

$$S_\zeta = \left\{ \zeta \in R: \|\zeta\| \leq \frac{2\Gamma \|P\|}{\kappa_{min}(Q)} \right\} \text{ where } \zeta = \begin{bmatrix} e_\eta \\ e_\eta \end{bmatrix}$$

represents the error matrix. Error dynamics (19) can be written as

$$\dot{\zeta} = A_C \zeta + \chi \quad (23)$$

$$\text{where } \zeta = \begin{bmatrix} e_\eta \\ \dot{e}_\eta \end{bmatrix}, \dot{\zeta} = \begin{bmatrix} \dot{e}_\eta \\ \ddot{e}_\eta \end{bmatrix}, A_C = \begin{bmatrix} 0 & 1 \\ -A_2 & -A_1 \end{bmatrix} \zeta,$$

$$\chi = \begin{bmatrix} 0 \\ -\hat{M}^{-1} Y e_\phi - \hat{M}^{-1} d \end{bmatrix}.$$

A Lyapunov function candidate is considered as follows:

$$V(\zeta) = \frac{1}{2} \zeta^T P \zeta \quad (24)$$

where P is symmetric and positive definite. From Equation (24)

$$\kappa_{min}(P) \|\zeta\|^2 \leq V(\zeta) \leq \kappa_{max}(P) \|\zeta\|^2 \quad (25)$$

The time derivative of the Lyapunov function is obtained as

$$\begin{aligned} \dot{V}(\zeta) &= \zeta^T P \dot{\zeta} + \dot{\zeta}^T P \zeta \\ &= \zeta^T P (A_C \zeta + \chi) + (A_C \zeta + \chi)^T P \zeta \\ &= \zeta^T P A_C \zeta + \zeta^T P \chi + \zeta^T A_C^T P \zeta + \chi^T P \zeta \\ &= \zeta^T (P A_C + A_C^T P) \zeta + 2 \chi^T P \zeta \end{aligned} \quad (26)$$

By design, we can ensure that

$$P A_C + A_C^T P = -Q \quad (27)$$

Then, Equation (25) becomes

$$\dot{V} = -\zeta^T Q \zeta + 2 \chi^T P \zeta \leq -\kappa_{min}(Q) \|\zeta\|^2 + 2 \|\chi\| \|P\| \|\zeta\| \quad (28)$$

Now,

$$\begin{aligned} \|\chi\| &= \left\| \begin{bmatrix} 0 \\ -\hat{M}^{-1} Y e_\phi - \hat{M}^{-1} T_E \end{bmatrix} \right\| \\ &\leq \|\hat{M}^{-1}\| (\|Y e_\phi\| + \|T_E\|) \\ &\leq \Gamma (\|Y e_\phi\| + \|T_E\|) \\ &\leq -\kappa_{min}(Q) \|\zeta\|^2 + 2\Gamma \|P\| \|\zeta\| \\ &\leq -\kappa_{min}(Q) \|\zeta\| \left(\|\zeta\| - \frac{2\Gamma \|P\|}{\kappa_{min}(Q)} \right) \end{aligned} \quad (29)$$

Hence

$$\|\zeta\| \leq \frac{2\Gamma \|P\|}{\kappa_{min}(Q)} \quad (30)$$

In Equation (30), $\frac{2\Gamma}{\kappa_{min}(Q)}$ is a positive constant, and $\|P\|$ is positively bounded. Thus, it can be concluded that the system is ultimately bounded by the Lyapunov stability theory within the range given by Equation (30). This confirms the feasibility condition (Lemma 2) of theorem (T1).

Next, as stated in the stability theorem (T1), the proof of stability requires knowledge of cost detectability, defined as follows:

Lemma 4: Cost Detectability: A cost function $\mathfrak{F}(t)$ is considered cost detectable if it fulfills the conditions given as follows [29]:

1. The function $\mathfrak{F}_i(t)$ monotonically increases in time t for all $(C_i, T, Y, \hat{\eta}_{des})$, $i = 1, 2, 3 \dots$
2. $\lim_{t \rightarrow \infty} \mathfrak{F}_i(t)$ remains uniformly bounded for all $(C_i, T, Y, \hat{\eta}_{des})$, $i = 1, 2, 3 \dots$ when C_i is stabilizing.

The cost function considered is

$$\mathfrak{F}(t) = \frac{\|\hat{e}_\eta\|^2 + \alpha \|T\|^2}{\|\hat{\eta}_{des}\|^2 + \rho} \quad (31)$$

$\alpha, \rho > 0$ are positive constants. $\hat{\eta}_{des}$ represents the fictitious reference and the fictitious error $\hat{e}_\eta = \hat{\eta}_{des} - \eta$ is the deviation of output from the fictitious reference.

To prove that $\mathfrak{F}(t)$ is monotonically increasing in time, equation (31) is differentiated w.r.t time t as follows:

$$\begin{aligned} \dot{\mathfrak{F}}(t) &= \frac{d}{dt} \left(\frac{\|\hat{e}_\eta\|^2 + \alpha \|T\|^2}{\|\hat{\eta}_{des}\|^2 + \rho} \right) \\ &= \frac{d}{dt} \left(\frac{\left\{ \left(\int_0^\infty |\hat{e}_\eta|^2 dt \right)^{\frac{1}{2}} \right\}^2 + \alpha \left\{ \left(\int_0^\infty |T|^2 dt \right)^{\frac{1}{2}} \right\}^2}{\left\{ \left(\int_0^\infty |\hat{\eta}_{des}|^2 dt \right)^{\frac{1}{2}} \right\}^2 + \rho} \right) \\ &= \frac{d}{dt} \left(\frac{\int_0^\infty |\hat{e}_\eta|^2 dt + \alpha \int_0^\infty |T|^2 dt}{\int_0^\infty |\hat{\eta}_{des}|^2 dt + \rho} \right) \\ &= \frac{\left(\int_0^\infty |\hat{\eta}_{des}|^2 dt + \rho \right) \frac{d}{dt} \left\{ \left(\int_0^\infty |\hat{e}_\eta|^2 dt \right) + \alpha \left(\int_0^\infty |T|^2 dt \right) \right\}}{- \left\{ \left(\int_0^\infty |\hat{e}_\eta|^2 dt \right) + \alpha \left(\int_0^\infty |T|^2 dt \right) \right\} \frac{d}{dt} \left(\int_0^\infty |\hat{\eta}_{des}|^2 dt + \rho \right)} \\ &= \frac{\left(\int_0^\infty |\hat{\eta}_{des}|^2 dt + \rho \right) \left(|\dot{\hat{e}}_\eta|^2 + \alpha |T|^2 \right) - \left(\int_0^\infty |\hat{e}_\eta|^2 dt + \alpha \int_0^\infty |T|^2 dt \right) |\dot{\hat{\eta}}_{des}|^2}{\left(\int_0^\infty |\hat{\eta}_{des}|^2 dt + \rho \right)^2} \\ &= \frac{\left(\|\hat{\eta}_{des}\|^2 + \rho \right) \left(|\dot{\hat{e}}_\eta|^2 + \alpha |T|^2 \right) - \left(\|\hat{e}_\eta\|^2 + \alpha \|T\|^2 \right) |\dot{\hat{\eta}}_{des}|^2}{\left(\|\hat{\eta}_{des}\|^2 + \rho \right)^2} \\ &= \frac{\left(\|\hat{\eta}_{des}\|^2 + \rho \right) \left(|\dot{\hat{e}}_\eta|^2 + \alpha |T|^2 \right) - \frac{\|\hat{e}_\eta\|^2 \|\dot{\hat{\eta}}_{des}\|^2}{\left(\|\hat{\eta}_{des}\|^2 + \rho \right)^2} - \frac{\alpha \|T\|^2 \|\dot{\hat{\eta}}_{des}\|^2}{\left(\|\hat{\eta}_{des}\|^2 + \rho \right)^2}}{\left(\|\hat{\eta}_{des}\|^2 + \rho \right)^2} \\ &= \frac{|\dot{\hat{e}}_\eta|^2 + \alpha |T|^2}{\|\hat{\eta}_{des}\|^2 + \rho} - \frac{\|\hat{e}_\eta\|^2 \|\dot{\hat{\eta}}_{des}\|^2}{\left(\|\hat{\eta}_{des}\|^2 + \rho \right)^2} - \frac{\alpha \|T\|^2 \|\dot{\hat{\eta}}_{des}\|^2}{\left(\|\hat{\eta}_{des}\|^2 + \rho \right)^2} \end{aligned} \quad (32)$$

Since, $\frac{\|\hat{e}_\eta\|^2 \|\dot{\hat{\eta}}_{des}\|^2}{\left(\|\hat{\eta}_{des}\|^2 + \rho \right)^2} \geq 0$ and $\frac{\alpha \|T\|^2 \|\dot{\hat{\eta}}_{des}\|^2}{\left(\|\hat{\eta}_{des}\|^2 + \rho \right)^2} \geq 0$

Therefore,

$$\dot{\mathfrak{F}}(t) \leq \frac{|\dot{\hat{e}}_\eta|^2 + \alpha |T|^2}{\|\hat{\eta}_{des}\|^2 + \rho} \quad (33)$$

Hence, $0 \leq \mathfrak{F}(t) \leq \frac{|\dot{\hat{e}}_\eta|^2 + \alpha |T|^2}{\|\hat{\eta}_{des}\|^2 + \rho}$ for all $(C_i, T, Y, \hat{\eta}_{des})$, $i = 1, 2, 3 \dots$

This confirms the cost detectability of $\mathfrak{F}(t)$ which by theorem (T1) fulfills a condition of stability. As the selection of the unfalsified controller depends on minimizing the cost function that depends on the actual and fictitious errors, the convergence of the errors can be assured. Moreover, the candidate set of controllers is generated using the lower

and upper bounds of the unknown parameters, which in any case confirms the boundedness of the estimates. The controller $C = C_f$ satisfies $\mathfrak{F}(t)$ and remains unfalsified at $t = \tau_f$ thus results in

$$\lim_{t \rightarrow \tau_f} \|\hat{\eta}_{des_f} - \eta_{des}\| = 0 \quad (34)$$

where $\hat{\eta}_{des_f}$ is the fictitious reference for controller $C = C_f$

Hence, by Equation (34), and by the arguments stated above, it is concluded that the control system is stable.

4.5. Finiteness of Parameter Switching

Switching of controllers depending on the attainment of the minimum cost function is performed by the following algorithm:

Hysteresis Switching Algorithm- $\Gamma_k \in R$ is a continuous logic input signal and δ is the output switching signal. δ and k belong to the normed vector space K . If at $t = t_0$, $\delta(0) = \arg \min_{k \in K} \{ \Gamma_k(0) \}$ and at some subsequent time $t = t_m$, δ is switched to $l \in K$. In this scenario case δ remains constant for time $t_{m+1} > t_m$ such that $(1 + n) \min \{ \Gamma_k(t_{m+1}) \} \leq \Gamma_l(t_m)$, n being the hysteresis constant. This generates a piecewise constant signal δ [30]. If Γ_k is uniformly bounded and $\Gamma_k \geq \omega$, such that $\omega > 0$, $\forall k \in K$ and all $t \geq 0$, the switching remains finite.

The monotonically decreasing set of unfalsified controllers bounded below by an empty set ensures a finite amount of switching among controllers. If there are n number of candidate controllers and at the minimum one stable controller satisfies the specified performance criteria, then by the algorithm stated above, after a maximum of $n-1$ switches the convergence of the switching of unfalsified controllers can be assured.

5. Results

The proposed controller design is applied to the system in Equation (7), and its performance is assessed via simulation in MATLAB/SIMULINK. The system parameters are described as follows:

$$M = \begin{bmatrix} M_{11} & 0 & 0 & 0 \\ 0 & M_{22} & 0 & 0 \\ 0 & 0 & M_{33} & 0 \\ 0 & 0 & 0 & M_{44} \end{bmatrix}, D = \begin{bmatrix} D_{11} & 0 & 0 & 0 \\ 0 & D_{22} & 0 & 0 \\ 0 & 0 & D_{33} & 0 \\ 0 & 0 & 0 & D_{44} \end{bmatrix}, \eta = \begin{bmatrix} x \\ y \\ z \\ \psi \end{bmatrix}, \text{ and } T = \begin{bmatrix} T_x \\ T_y \\ T_z \\ T_\psi \end{bmatrix} \quad (35)$$

The regressor matrix is defined as

$$Y(\eta, \dot{\eta}, \ddot{\eta}) \Phi^T = \begin{bmatrix} \ddot{x} & |\dot{x}| \dot{x} & 0 & 0 & 0 & 0 & 0 & 0 \\ 0 & 0 & \ddot{y} & |\dot{y}| \dot{y} & 0 & 0 & 0 & 0 \\ 0 & 0 & 0 & 0 & \ddot{z} & |\dot{z}| \dot{z} & 0 & 0 \\ 0 & 0 & 0 & 0 & 0 & 0 & \ddot{\psi} & |\dot{\psi}| \dot{\psi} \end{bmatrix} \begin{bmatrix} M_{11} \\ D_{11} \\ M_{22} \\ D_{22} \\ M_{33} \\ D_{33} \\ M_{44} \\ D_{44} \end{bmatrix} \quad (36)$$

Let the desired trajectory be

$$\eta_{des} = \begin{bmatrix} x_{des} \\ y_{des} \\ z_{des} \\ \psi_{des} \end{bmatrix} = \begin{bmatrix} 10 \sin(t) \\ 10 \cos(t) \\ 10 \\ \frac{\pi}{3} \end{bmatrix} \quad (37)$$

The initial values of the states of the AUV are taken as $\eta(0) = [1,1,0.5,0.1]^T$ and $\dot{\eta}(0) = [0,0,0,0]^T$. For the CTC, the control gain values are $\Lambda_1 = 25$ and $\Lambda_2 = 625$. The nominal values of these parameters are taken from [31], and a minimum and maximum bound on the variation of these parameter values is considered based on the nominal values. The nominal, minimum, and maximum values for each parameter are given in Tables 1 and 2. Next, a set of 20 random values is generated between the upper and lower bounds for each $[\phi_1, \dots, \phi_8]^T$ using the MATLAB function. These 20 random values, applied to the control law in Equation (13), constitute the 20 candidates of the controller bank. Using these values of $C_i, i = 1,2, \dots, 20$ a fictitious reference $\hat{\eta}_{des}$ is derived for each candidate controller using the relation in Equation (20). The cost function $\mathfrak{F}(t)$ considered is the minimum of the performance specification $T_{spec}(\hat{\eta}_{des}, T, Y)$, i.e. $\mathfrak{F}(t) = \min T_{spec}(\hat{\eta}_{des}, T, Y)$. The performance specifications considered are given below.

$$T_{spec} = \frac{W_1 \|\hat{\eta}_{des}(t) - \eta(t)\|^2 + W_2 \|T(t)\|^2}{W_3 \|\hat{\eta}_{des}(t)\|^2 + \rho} \quad (38)$$

where $W_1, W_2,$ and W_3 are weighting factors and ρ is a constant. The results satisfying the performance criterion (38) are presented in this paper.

The unknown parameters are estimated using the unfalification algorithm, which gives the near-optimal values of the aforementioned parameters. The parameters $\phi_1,$

$\phi_3, \phi_5,$ and ϕ_7 are mass parameters of the system and are plotted against their nominal values, as given in Table 1. The parameters $\phi_2, \phi_4, \phi_6,$ and ϕ_8 are damping parameters, as shown in Table 2. The estimated values obtained by minimizing the performance specification in (38) are also presented in Tables 1 and 2 along with the estimation error. The switching in the parameter values of $\phi_1, \phi_3, \phi_5,$ and ϕ_7 can be observed in Figure 3.

The switching in the values of $\phi_2, \phi_4, \phi_6,$ and ϕ_8 is shown in Figure 4.

As the algorithm runs for a complete iteration, the change in plant dynamics changes parameter values. Hence, causing the switching in parameter values. It is observed that the parameter estimates obtained are quite close to the nominal values of the parameters. Due to the inclusion of the norm of the control input term, switching shows a high variation during the transient period. The AUV is effectively guided by the controller that remains unfalsified to follow the specified trajectory, thereby achieving the control objective. Figure 5 shows the tracking at each DOF, while Figure 6 depicts the circular trajectory plot.

In Figure 7, the error convergence plot is shown.

The results obtained are compared with those of the classical adaptive control design proposed in [31]. The tracking results presented in [31] show absolute convergence in 10 s, whereas in the proposed design, as evident from the results presented, absolute convergence is attained in 7 s. Thus, confirming faster and better convergence. Furthermore, the absence of parameter update dynamics in the closed-loop system, which is a characteristic of other adaptive methods, results in reduced computational complexity, providing an additional advantage in the proposed design.

Table 1. Unknown mass parameters

Sl. No.	Unknown parameter	Mass parameter	Nominal value (kg)	Min. value	Max. value	Estimated value	Absolute error
1	ϕ_1	M_{11}	100	90	110	98.04	1.96
2	ϕ_3	M_{22}	109	100	120	116.8	7.8
3	ϕ_5	M_{33}	125	115	135	127.2	2.2
4	ϕ_7	M_{44}	28.8	20	40	21.93	6.87

Table 2. Unknown damping parameters

Sl. No.	Unknown parameter	Damping parameter	Nominal value (kg/s)	Min. value	Max. value	Estimated value	Absolute error
1	ϕ_2	D_{11}	10	1	20	3.5	6.5
2	ϕ_4	D_{22}	400.18	390	410	393.5	6.48
3	ϕ_6	D_{33}	10	1	20	18.84	8.84
4	ϕ_8	D_{44}	1.8	1	3	2.95	1.15

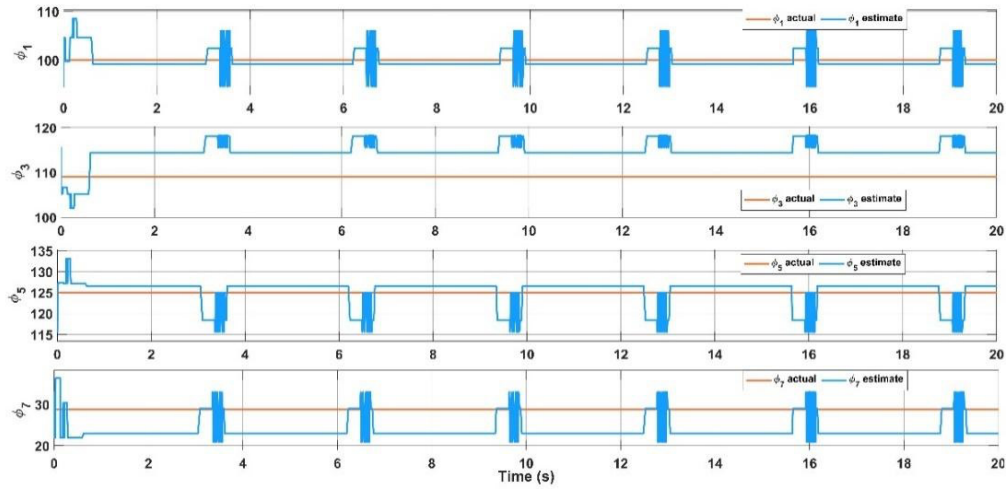


Figure 3. Parameter switching ($\phi_1 - \hat{\phi}_1, \phi_3 - \hat{\phi}_3, \phi_5 - \hat{\phi}_5, \phi_7 - \hat{\phi}_7$)

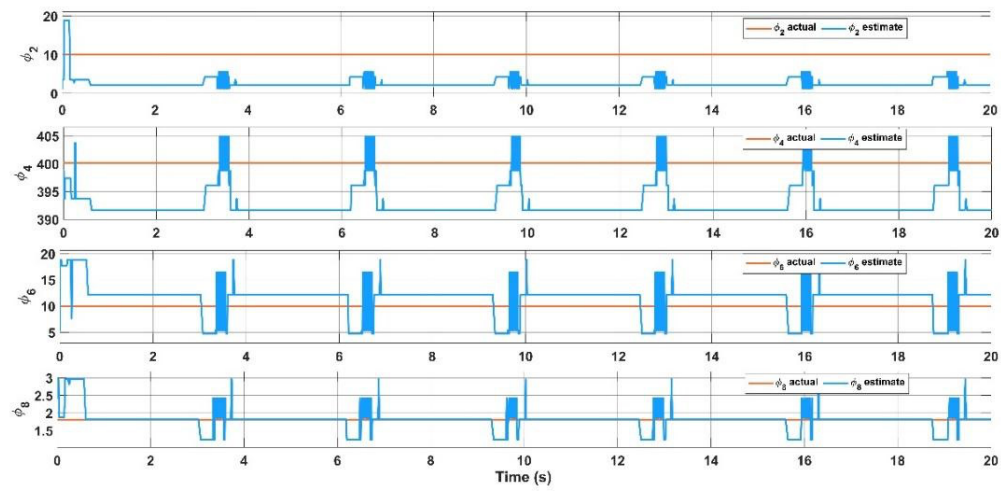


Figure 4. Parameter switching ($\phi_2 - \hat{\phi}_2, \phi_4 - \hat{\phi}_4, \phi_6 - \hat{\phi}_6, \phi_8 - \hat{\phi}_8$)

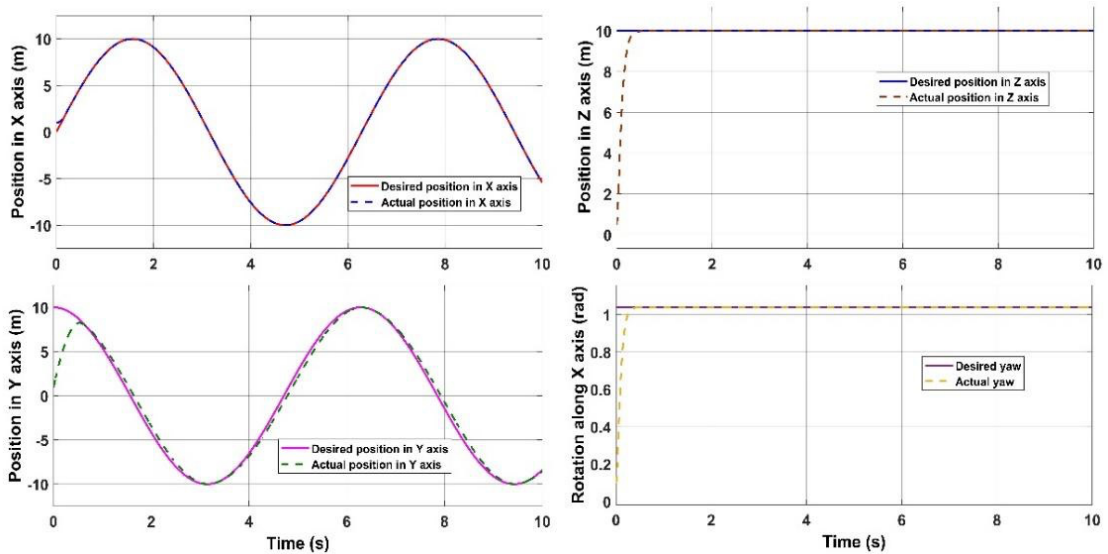


Figure 5. Trajectory tracking along the X, Y, and Z axes

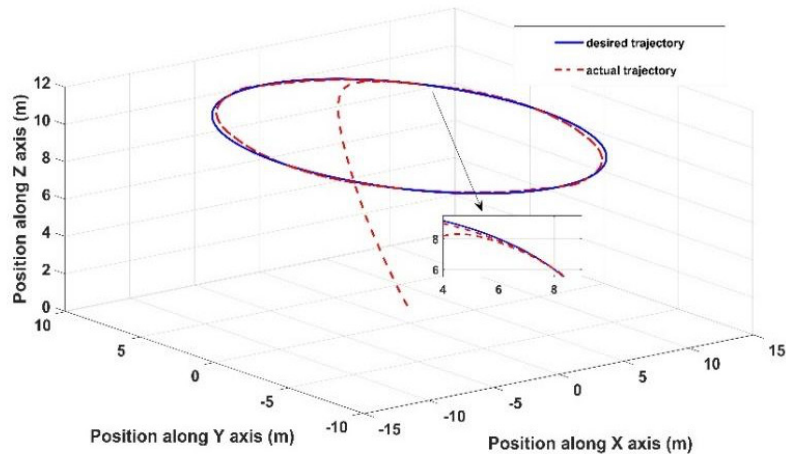


Figure 6. Circular trajectory tracking

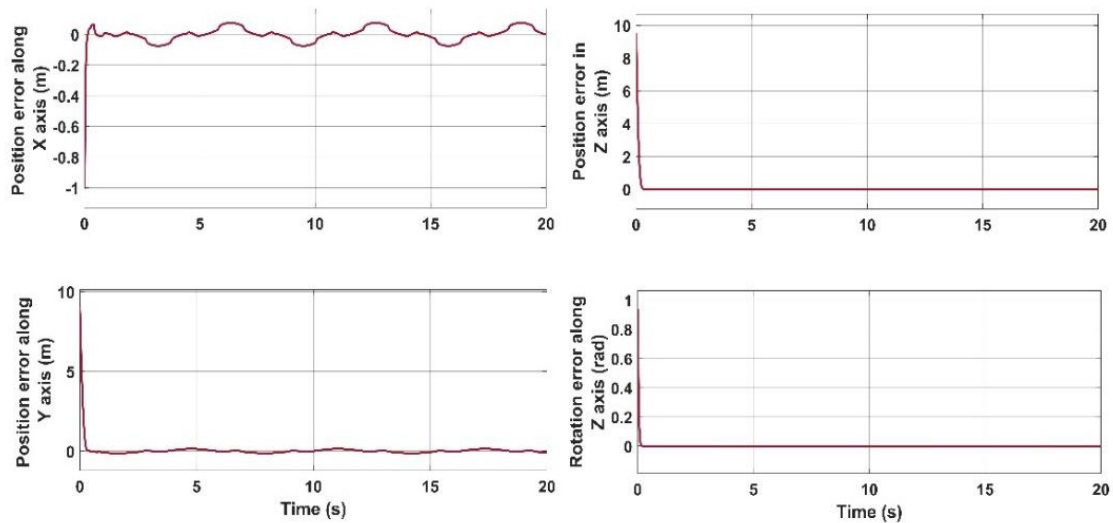


Figure 7. Error convergence in adaptive unfalsified control

6. Conclusion

The functioning of an AUV is likely to be affected by its physical non-linearities and environmental disturbances. Thus, it is favorable to use an adaptive plus data-driven method to control an AUV. This paper proposes adaptive control using the method of falsification with real-time input-output data. The approach utilizes measured information of input and output to select a controller from the candidate set. The plant used here is unknown, and the method uses the concept of a fictitious reference to obtain the parameter estimates. Near-optimal values of the parameter estimates are obtained by minimizing a designated cost function that considers the performance criteria. The controller utilizes these estimated values of parameters to guide the AUV toward the reference trajectory.

Simulation results verify the adaptiveness of the controller in estimating unknown parameters and prove its efficacy in attaining tracking objectives. The proposed design of the controller has also been corroborated with stability analysis and proof. The results have been substantiated with comparative results from another established method. In future work, it is planned to broaden the controller's scope by incorporating robust controllers into the controller bank and applying it to higher DOF robotic systems, thereby establishing the robustness of the controller design. In addition, in this work, a fixed convex set of candidates has been used for parameter estimation. This can be upgraded for non-convex sets using the latest optimization techniques.

Authorship Contributions

Concept design: T. Rasul, and K. Mukherjee, Data Collection or Processing: T. Rasul, Analysis or Interpretation: T. Rasul, Literature Review: T. Rasul, Writing, Reviewing and Editing: T. Rasul, and K. Mukherjee.

Funding: The authors did not receive any financial support for the research, authorship and /or publication of this article.

References

- [1] M. Jun, and M. G. Safonov, "Automatic PID tuning: an application of unfalsified control". in *Proceedings of the International Symposium on Computer Aided Control System Design*, Hawaii, USA, 1999.
- [2] S. Liu, D. Wang, and E. Poh, "Nonlinear adaptive observer design for tracking control of AUVs in wave disturbance condition," *OCEANS 2006, Asia Pacific*, pp. 1-8.
- [3] K. M. Tan, A. Anvar, and T.F. Lu, "Autonomous underwater vehicle (AUV) dynamics modelling and performance evaluation". *World Academy of Science, Engineering and Technology International Journal of Mechanical and Mechatronics Engineering*, vol. 6, Dec 2012.
- [4] O. Hassanein, S. G. Anavatti, S. Hyungbo, and T. Ray, "Model-based adaptive control system for autonomous underwater vehicles". *Ocean Engineering*, vol. 127, pp. 58-69, Nov 2016.
- [5] C. Silvestre, and A. Pascoal, "Nonlinear H_∞ optimal control scheme for an underwater vehicle with regional function formulation". *Journal of Applied Mathematics*, 2013.
- [6] S. Liu et al., "Nonlinear adaptive observer design for tracking control of AUVs in wave disturbance condition," in *Proceedings of 2004 IEEE International Conference on Intelligent Robots and Systems*, Japan, 2004.
- [7] K. Mukherjee, I. N. Kar, and R. K. P. Bhatt, "Ocean Waves: A disturbance observer approach for an autonomous underwater vehicle". *OCEANS 2019 Marseille*.
- [8] M. G. Safonov, and T. C. Tsao, "The unfalsified control concept: A direct path from experiment to controller," *Feedback Control, Nonlinear Systems, and Complexity*, vol. 202, pp. 196-214, 1995.
- [9] D. J. Leith, and W. E. Leithead, "Appropriate realization of gain-scheduled controllers with application to wind turbine regulation," *International Journal of Control*, vol. 65, pp. 223-248, 1996.
- [10] D. J. Leith, and W. E. Leithead, "Survey of gain-scheduling analysis and design". *International Journal of Control*, vol. 73, pp. 1001-1025, 2000.
- [11] T. C. Tsao, and M. G. Safonov, "Unfalsified direct adaptive control of a two-link robot arm". *International Journal of Adaptive Control and Signal Processing*, Apr 2001.
- [12] M. G. Safonov, and S. Y. Cheong, "Unfalsified Control: Theory and Applications". In *IEEE Conference on Decision and Control, San Diego, CA Dec 2006*.
- [13] M. G. Safonov, "Data-driven robust control design: Unfalsified Control". In *Proceedings of NATO Lecture Series 236, Robust Integrated Control Systems Design Methods for 21st Century Military Applications*, NATO Research and Technology Office, 2003.
- [14] C. Manuelli, S. G. Cheong, E. Mosca, and M. G. Safonov, "Stability of unfalsified adaptive control with non-SCLI controllers and related performance under different prior knowledge". In *2007 European Control Conference (ECC), Kos, Greece, 2007*, pp. 702-708.
- [15] A. Paul, M. Stefanovic, M. G. Safonov, and M. Akar, "Multi-controller adaptive control (MCAC) for a tracking problem using an unfalsification approach". In *Proceedings of the 44th IEEE Conference on Decision and Control*, pp. 4815-4820, 2005.
- [16] F. B. Cabral, and M. G. Safonov, "Unfalsified model reference adaptive control using the ellipsoid algorithm". In *Proceedings of IEEE Conference on Decision and Control*, 2013.
- [17] R. S. Sanchez-Pena, P. Colmegna, and F. Bianchi, "Unfalsified control based on the H_∞ controller parametrization". *International Journal of Systems Science*, vol. 46, pp. 1-12, Dec 2014.
- [18] F. Previdi, T. Schauer, S. M. Savaresi, and K. J. Hunt, "Data-driven control design for neuroprostheses: a virtual reference feedback tuning (VRFT) approach". *IEEE Transactions on Control Systems Technology*, vol. 12, pp. 176-182, Jan 2004.
- [19] Jing Wang and Yue Wang and Liulin Cao and Qibing Jin, "Adaptive iterative learning control based on unfalsified strategy for Chylla-Haase reactor". *IEEE/CAA Journal of Automatica Sinica*, vol. 1, 2014.
- [20] V. Hassani, T. F. Onstein, and A. M. Pascoal, "Application of data-driven control to dynamic positioning". *IFAC-PapersOnLine*, vol. 50, pp. 12392-12397, 2017.
- [21] J. Das, et al. "Data-driven robotic sampling for marine ecosystem monitoring". *The International Journal of Robotics Research*, vol. 34, pp. 1435-1452, Aug 2015.
- [22] T. O. Fossum, "Intelligent autonomous underwater vehicles: a review of AUV autonomy and data-driven sample strategies". PhD Dissertation from Applied Underwater Robotic Laboratory, Norwegian University of Science and Technology, Trondheim, Norway, 2016.
- [23] Y.-C. Sung, S. V. Patil, and M. G. Safonov, "Data-driven H_∞ loop-shaping controller design". *International Journal of Robust and Nonlinear Control*, vol. 28, pp. 3678-3693, Jul 2016.
- [24] S. V. Patil, Y.-C. Sung, and M. G. Safonov, "Nonlinear unfalsified adaptive control with bumpless transfer and reset". *IFAC-PapersOnLine*, vol. 49, pp. 1066-1072, 2016.
- [25] Y.-C. Sung, S. V. Patil, and M. G. Safonov, "Robustness of uncertain switching nonlinear feedback systems against large time-variation". *IEEE Transactions on Automatic Control*, vol. 67, pp. 993-1000, Feb 2022.
- [26] S. V. Patil, Y.-C. Sung, and M. G. Safonov, "Unfalsified adaptive control for nonlinear time-varying plants". *IEEE Transactions on Automatic Control*, vol. 67, pp. 3892-3904, Aug 2022.
- [27] T. I. Fossen, *Guidance and control of ocean vehicles*, John Wiley and Sons, 1994.
- [28] R. Wang, and M. G. Safonov, "Stability of unfalsified adaptive control using multiple controllers". *American Control Conference*, 2005.

- [29] M. Stefanovic, A. Paul, and M. G. Safonov, "Safe adaptive switching through infinite controller set: Stability and convergence". *IFAC Proceedings Volumes*, vol. 38, pp. 73-78, 2005.
- [30] J. P. Hespanha, *Logic-based switching algorithms in control*, Yale University, 1998.
- [31] B. K. Sahu, and B. Subudhi, "Adaptive tracking control of an autonomous underwater vehicle". *International Journal of Automation and Computing*, vol. 11, pp. 299-307, Mar 2015.